Binary evolution in a nutshell
# (BEiaNS)
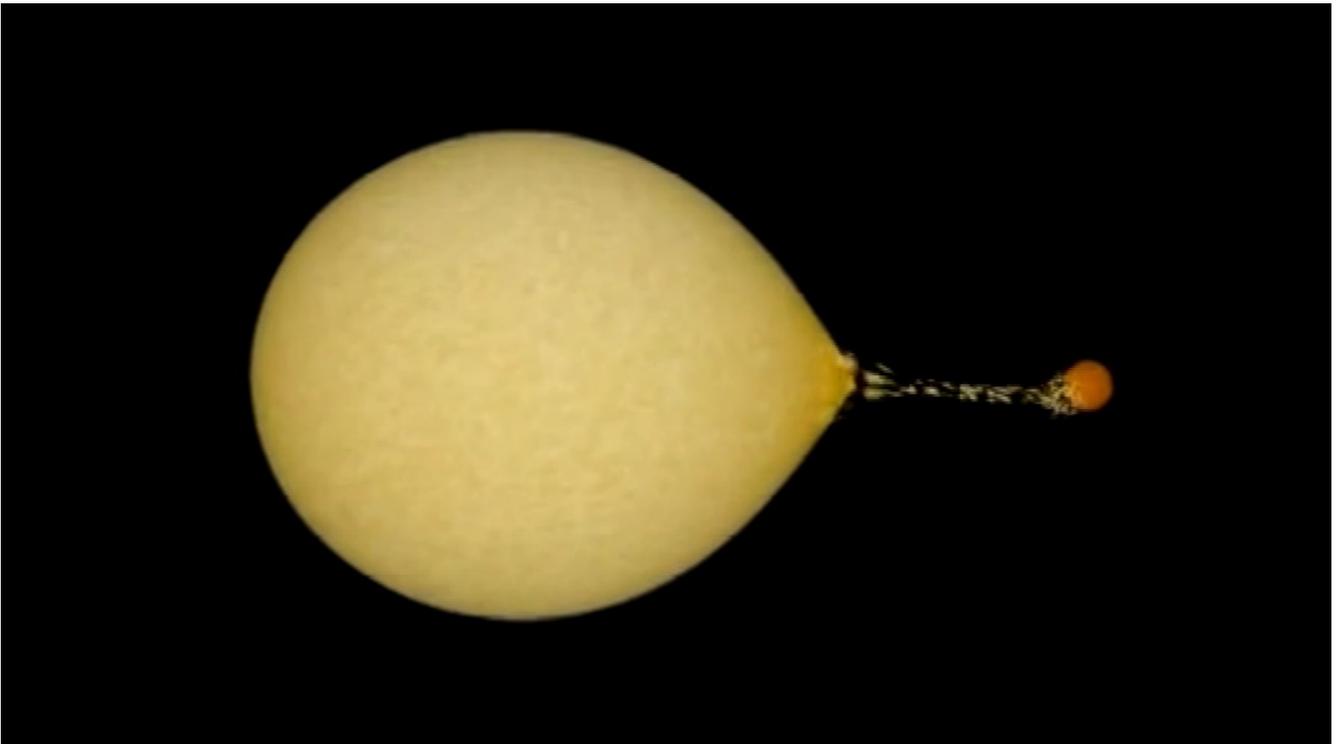
Marc van der Sluys
Department of Physics,
Utrecht University/Nikhef,
the Netherlands
June 2, 2025

Cover image:
The image on the cover shows a still from an animation that represents a detailed model of a stellar binary during its phase of stable mass transfer. The model was calculated using the "Eggleton code", and the physical output parameters from that calculation were fed into a graphical simulation program called BinSim, by R. Hynes of LSU.

Contents

Preface

This document contains the most important equations used in binary evolution. It was created as a cheat sheet for myself, but I also use it for teaching. If you find it useful, you are welcome to use it. If you have any questions or comments, please send me an email. The most recent version of this document can be found at `https://www.nikhef.nl/~sluys/index.php?title=BEiaNS` in both A4 and Letter format.

1 Stellar properties

1.1 Mass-radius and mass-luminosity relations for main-sequence stars

For main-sequence stars, the relation

$$\frac{R}{R_\odot} \approx \left(\frac{M}{M_\odot} \right)^n \tag{1.1}$$

gives a decent description of the radius of the star as a function of its mass for $M \sim 0.12-25\,M_\odot$ (although not so great around $M \sim 2.5\,M_\odot$), with $n \approx 1$ for $M \lesssim 1\,M_\odot$ and $n \approx 0.6$ for $M \gtrsim 1\,M_\odot$.

Even tighter is the fit for the mass-luminosity relation of main-sequence stars:

$$\frac{L}{L_\odot} \approx \left(\frac{M}{M_\odot} \right)^{3.8} \tag{1.2}$$

for $M \sim 0.2 - 25\,M_\odot$.

1.2 Mass-radius relation for white dwarfs, neutron stars and black holes

The radius of a white dwarf can be found as a function of its mass using

$$\left(\frac{R_{\rm wd}}{R_\odot} \right) \approx 0.01125 \left[\left(\frac{M_{\rm wd}}{1.454 M_\odot} \right)^{-2/3} - \left(\frac{M_{\rm wd}}{1.454 M_\odot} \right)^{2/3} \right]^{1/2} \tag{1.3}$$

(Nauenberg, 1972, Eq. 27, with $\mu = 2$).

A reasonable guess for the radius of a neutron star is

$$R_{\rm ns} \approx 12\,{\rm km}, \tag{1.4}$$

although models range between ~ 10 and $15\,{\rm km}$ and may go as low as $7\,{\rm km}$, depending on the equation of state assumed.

The radius of a non-spinning black hole is given by its Schwarzschild radius:

$$R_{\rm s} = \frac{2GM}{c^2}. \tag{1.5}$$

1.3 Conditions in stellar centres

For the pressure in the centre of a star, we can roughly estimate

$$P_{\rm c} \sim \frac{GM}{R}\bar{\rho} \sim \frac{3GM^2}{4\pi R^4}, \tag{1.6}$$

where $\bar{\rho}$ is the mean density of the star.

Applying the ideal-gas law, we can write the central temperature equally roughly as

$$T_{\rm c} \sim \frac{\mu m_H}{k} \frac{GM}{R} \frac{\bar{\rho}}{\rho_{\rm c}}. \tag{1.7}$$

From radiation equilibrium, we can estimate the luminosity of the star as

$$L \sim \frac{64\pi^2}{9} \frac{\sigma}{\bar{\kappa}} \frac{R^4}{M} T_c^4 \sim \frac{64\pi^2}{9} \frac{\sigma}{\bar{\kappa}} \left(\frac{\mu m_H G}{k}\right)^4 \left(\frac{\bar{\rho}}{\rho_c}\right)^4 M^3, \tag{1.8}$$

where $\bar{\kappa}$ is the mean opacity and we used Eq. 1.7 in the second step.

1.4 Stellar timescales

1.4.1 Dynamical timescale

An estimate of the dynamical timescale of a star can be given by estimating how long it would take a star of given mass and radius, and consisting of particles that do not interact other than to gravity, to collapse. This is also known as the *free-fall* timescale. From the gravitational acceleration of these particles $\frac{d^2 R}{dt^2} \sim -\frac{GM}{R^2}$ and very roughly assuming that this is equal to $\frac{-R}{\tau_{\rm dyn}^2}$, we find

$$\tau_{\rm dyn} \sim \tau_{\rm ff} \sim \sqrt{\frac{R^3}{GM}} \approx 1.6 \times 10^3 \,\mathrm{s} \left(\frac{M}{M_\odot}\right)^{-1/2} \left(\frac{R}{R_\odot}\right)^{3/2}, \tag{1.9}$$

or about 27 minutes for the Sun.

1.4.2 Thermal timescale

The thermal timescale is the timescale at which a star with given mass, radius and luminosity could radiate away its gravitational energy. This is often approximated by the *Kelvin-Helmholtz* timescale:

$$\tau_{\rm th} \sim \tau_{\rm KH} \sim \frac{E_{\rm th}}{L} \sim \frac{GM^2}{RL} \approx 3.1 \times 10^7 \,\mathrm{yr} \left(\frac{M}{M_\odot}\right)^2 \left(\frac{R}{R_\odot}\right)^{-1} \left(\frac{L}{L_\odot}\right)^{-1}. \tag{1.10}$$

For giants (stars with a clear core-envelope structure), one often uses:

$$\tau_{\rm th} \sim \tau_{\rm KH} \sim \frac{GMM_{\rm env}}{RL} \approx 3.1 \times 10^7 \,\mathrm{yr} \left(\frac{M}{M_\odot}\right) \left(\frac{M_{\rm env}}{M_\odot}\right) \left(\frac{R}{R_\odot}\right)^{-1} \left(\frac{L}{L_\odot}\right)^{-1}. \tag{1.11}$$

1.4.3 Nuclear-evolution timescale

The nuclear-evolution timescale of a (main-sequence) star can be roughly estimated by the ratio of the amount of available "fuel" (its mass) and the rate and efficiency at which it is "burned" (its luminosity):

$$\tau_{\rm nuc} \sim 0.15 \frac{0.0069 M c^2}{L} \approx 1.5 \times 10^{10} \,\mathrm{yr} \left(\frac{M}{M_\odot}\right) \left(\frac{L}{L_\odot}\right)^{-1}, \tag{1.12}$$

where 0.15 is roughly the mass fraction of the Sun where hydrogen fusion can take place, and 0.0069 is the fraction of mass converted to energy in hydrogen fusion.[1] In reality, the Sun lives a bit shorter than 15 Gyr, mainly because its luminosity increases during its lifetime.

For main-sequence stars with masses between roughly $0.2\,M_\odot$ and $25\,M_\odot$, we can scale Eq. 1.2 with the nuclear-evolution timescale of the Sun gives an approximation of the nuclear-evolution timescale of a star with given mass:

$$\tau_{\rm nuc} \sim \frac{M}{L} \sim \tau_{\rm nuc,\odot} \left(\frac{M}{M_\odot}\right) \left(\frac{L}{L_\odot}\right)^{-1} \approx 10^{10} \,\mathrm{yr} \left(\frac{M}{M_\odot}\right) \left(\frac{L}{L_\odot}\right)^{-1} \approx 10^{10} \,\mathrm{yr} \left(\frac{M}{M_\odot}\right)^{-2.8}. \tag{1.13}$$

Here we made the assumption that the fraction of the stellar mass available for hydrogen fusion is the same for all stars. In reality, this may be much larger for more massive stars, for example because they have convective cores and can mix material from outside into the 'burning' region to be fused.

---

[1] $\frac{m_{\rm He4} - 2m_{\rm e} - 4m_{\rm p}}{4m_{\rm p}} \approx \frac{4.002603254 - 2 \cdot 5.48579909065e-4 - 4 \cdot 1.007276466621}{4 \cdot 1.007276466621} \approx -0.00685$, where the electron masses are subtracted to obtain the mass of the helium *nucleus*.
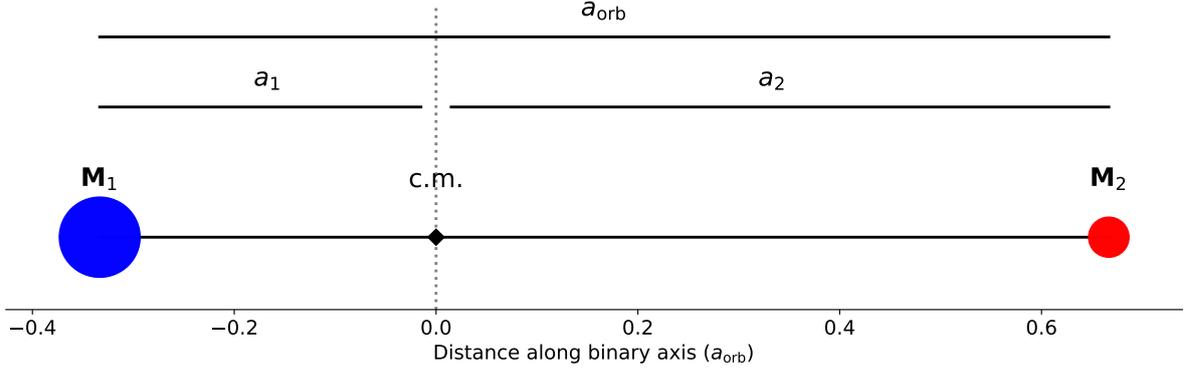
Figure 2.1: Schematic geometry of a binary with masses $M_1 = 2 M_2$, and orbital separation a_{orb}. The distances a_1, a_2, are from the binary members to the centre of mass (c.m.), which is also the rotation axis of the binary.

For evolutionary phases other than the main sequence, one could scale Eq. 1.13 with the energy efficiency of the nuclear reaction involved. However, this is only true for other core-burning phases, in which case a burning shell often provides a significant fraction (if not the majority) of the luminosity.

If the timescale is needed in the context of mass transfer, the relevant timescale is often that of the rate $\dot{R}$ of change of the stellar radius due to the nuclear evolution of the star. If a stellar-evolution code is available, so that R and hence $\dot{R}$ can be computed, one can use

$$\tau_{\text{nuc}} \approx \frac{R}{\dot{R}}. \tag{1.14}$$

Of course, this number is only meaningful if stellar evolution is indeed the drive for the change in radius. It is useless if for instance the star fills its Roche lobe.

2 Geometry of a binary star

Figure 2.1 shows a sketch of the geometry of a binary star. For most expressions below, I will assume a circular orbit. The subscript i denotes a binary component $(i = 1, 2)$; the subscript $(3 - i)$ indicates the *other* binary component.

2.1 Masses

The total mass M_{T}, mass ratio q and reduced mass μ of a binary are given by:

$$M_{\text{T}} = M_1 + M_2, \tag{2.1}$$

$$q_i = \frac{M_i}{M_{(3-i)}}, \tag{2.2}$$

and

$$\mu = \frac{M_1 M_2}{M_{\text{T}}}. \tag{2.3}$$

Note that

$$M_i = M_{\text{T}} \frac{q_i}{1 + q_i} = \frac{M_{\text{T}}}{1 + q_{(3-i)}} \tag{2.4}$$

2.2 Chirp mass and symmetric mass ratio

When working with gravitational waves (see Sect. 5.3), the *chirp mass* $\mathcal{M}$ and *symmetric mass ratio* $0 < \eta \leq 1$ are often used:

$$\eta = \frac{M_1 M_2}{M_{\text{T}}^2} = \frac{q}{(1 + q)^2}; \tag{2.5}$$

$$\mathcal{M} = M_\mathrm{T}\,\eta^{3/5} \;=\; \left(\frac{M_1 M_2}{M_\mathrm{T}^{1/3}}\right)^{3/5}. \tag{2.6}$$

To compute $0 < q \le 1$ from η, use

$$q = \frac{1 - \sqrt{1 - 4\eta}}{1 + \sqrt{1 - 4\eta}}. \tag{2.7}$$

2.3   Centre of mass

The distance to the centre of mass (c.m.) or rotation axis for each of the binary members (a_i, see Fig. 2.1 and Appendix A.2) is given by:

$$a_i = \frac{M_{(3-i)}}{M_\mathrm{T}}\,a, \tag{2.8}$$

$$\frac{a_1}{M_2} = \frac{a_2}{M_1} = \frac{a}{M_\mathrm{T}} \tag{2.9}$$

or

$$M_1\,a_1 = M_2\,a_2 = \mu\,a. \tag{2.10}$$

Note that

$$q_i = \frac{M_i}{M_{(3-i)}} = \frac{a_{(3-i)}}{a_i}. \tag{2.11}$$

2.4   Kepler's law

Kepler's law can be written as:

$$\omega^2 = \left(\frac{2\pi}{P}\right)^2 = \frac{GM_\mathrm{T}}{a^3}, \tag{2.12}$$

where $\vec{\omega} = \dfrac{\vec{r} \times \vec{v}}{r^2}$ is the *angular velocity* (or angular frequency; $\omega = 2\pi f$). From this, we can write

$$a = \left(\frac{GM_\mathrm{T}}{4\pi^2}\right)^{1/3}\,P^{2/3} \tag{2.13}$$

or

$$P = \left(\frac{4\pi^2}{GM_\mathrm{T}}\right)^{1/2}\,a^{3/2}. \tag{2.14}$$

See Appendix A.3 for a derivation of Kepler's law for a circular orbit.

3   The Roche potential

The gravitational and rotational potential in a frame corotating with the binary is called the Roche potential (see Figure 3.1), and defined as:

$$\Phi_\mathrm{Roche}(\vec{r}) = -\frac{GM_1}{|\vec{r} - \vec{r}_1|} - \frac{GM_2}{|\vec{r} - \vec{r}_2|} - \frac{1}{2}\left(\vec{\omega} \times \vec{r}\right)^2, \tag{3.1}$$

where $\vec{r}_1$ and $\vec{r}_2$ denote the positions of the two stars and the last term is the potential due to the centrifugal force (see Appendix A.4).

The acceleration and net force for a test mass m can be computed through the gradient of the potential

$$\vec{a} = \frac{\vec{F}}{m} = -\nabla\Phi_\mathrm{Roche}. \tag{3.2}$$

There are five points where the acceleration or net force on a test particle is zero, called the *Lagrangian points* or stationary points and denoted L_1 through L_5. L_1–L_3 are saddle points that lie on the binary
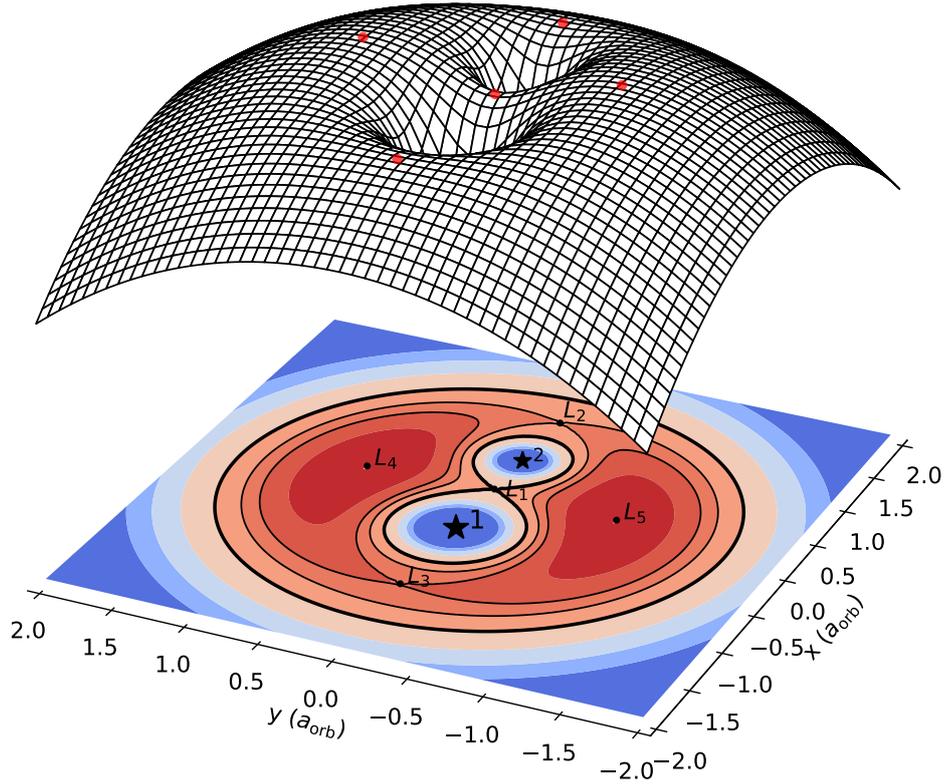
Figure 3.1: Three-dimensional representation of the Roche potential for a binary with $M_1 = 1\,M_\odot$, $M_2 = 0.5\,M_\odot$ and $P_{\mathrm{orb}} = 1\,\mathrm{day}$. The droplet-shaped areas in the equipotential plot on the bottom of the figure are the Roche lobes of the two stars (thick lines) — the more massive companion has the larger lobe. The points L_i are the Lagrangian points where forces cancel: L_1 between the two stars, L_2 and L_3 "behind" star 2 and star 1 respectively, and L_4 and L_5 to the sides. The Lagrangian points are also shown as unlabeled red dots in the 3D mesh. Spatial dimensions are expressed in terms of the orbital separation a_{orb}. Note that L_1 is *not* the centre of mass. Adapted from van der Sluys (2006).
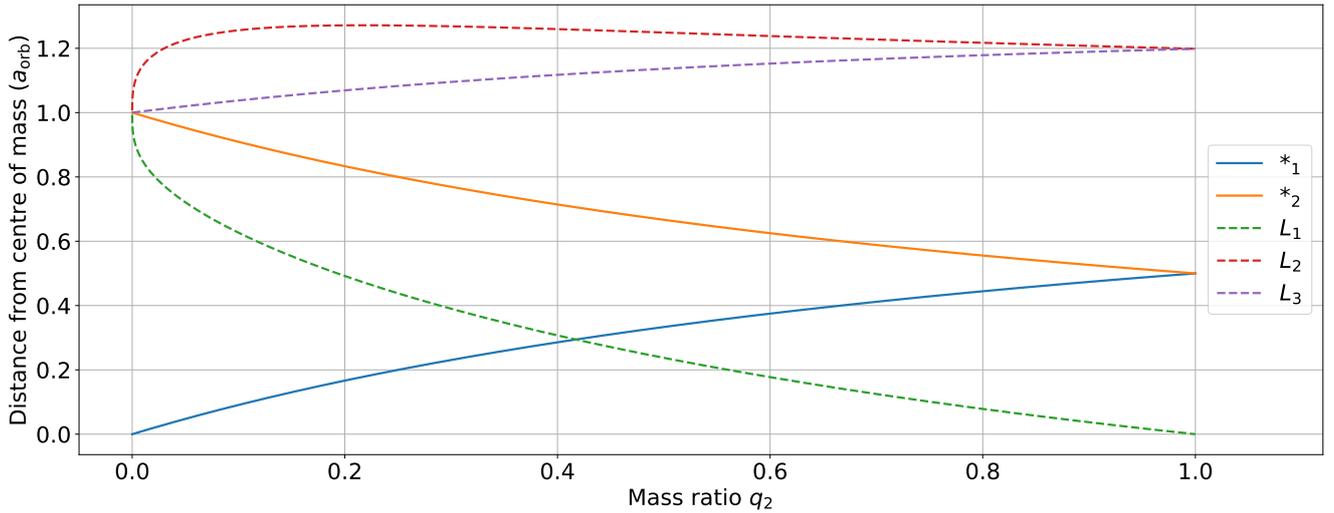
Figure 3.2: Distances to the centre of mass of the binary of the two stars ($*_1$, $*_2$) and the first three Lagrangian points ($L_1 - L_3$), expressed in terms of the orbital separation a_{orb} and as a function of the mass ratio $q_2 = M_2/M_1$. Four quantities change monotonically, but L_2 lies between $1.2\,a_{\mathrm{orb}}$ and $1.3\,a_{\mathrm{orb}}$ for most mass ratios and reaches a maximum of $\sim 1.27\,a_{\mathrm{orb}}$ around $q_2 \sim 0.218$. For $q_2 = 1$, $a_1 = a_2$ and $L_2 = L_3$, as expected for this symmetrical case, wheras $L_1 = 0$, since it lies at the centre of mass and on the rotation axis. Note that $L_1 - L_3$ converge very slowly to the location of star 2 as $q_2 \to 0$. For $q_2 = 0$, star 1 is the only remaining star, and hence at the centre of mass, whereas all other distances equal a_{orb}, which has become meaningless.

axis, as shown in Figure 3.1. Matter can be transferred from a Roche-lobe-filling star to its companion through L_1, and matter can be lost from the binary into a circumbinary disc through L_3 (behind the more massive star) and to infinity through L_2 (behind the lower-mass companion) if both stars fill their Roche lobes. L_4 and L_5 are maxima off-axis from L_1. The positions of the Lagrangian points can be found by computing the roots of Eq. 3.2, *i.e.* of the gradient of Eq. 3.1 (see Appendix A.5). The Lagrangian points L_1 through L_3 are of particular interest: mass transfer between the binary members happens through L_1, a circumbinary disc can be formed when matter escapes from L_3 and mass loss to infinity can happen through L_2. The distances between L_1, L_2 (as well as a_1, a_2) and the centre of mass are shown in Figure 3.2.

The Roche potential from Equation 3.1 can be written as

$$\Phi_{\mathrm{Roche}}(r) = -\frac{GM_{\mathrm{T}}}{a} \cdot f\left(\frac{r}{a}, q\right), \tag{3.3}$$

where the first term denotes the *scale* of the potential, which depends on the total mass and orbital separation, and the second term determines its *shape*, and which only depends on the mass ratio (see Appendix A.6).

Note that, because we're in a corotating frame,

$$\lim_{r \to \infty} -\frac{1}{2}\left(\vec{\omega} \times \vec{r}\right)^2 = -\infty.$$

This does not cause a problem, because the corotating frame does not extend far beyond the binary. Note also that a corotating frame is *not* an inertial frame! This results firstly in a *centrifugal force*. Secondly, particles that are *moving* w.r.t. a co-rotating frame will experience the fictitious Coriolis force:

$$\vec{F}_{\mathrm{c}} = -2m\left(\vec{\omega} \times \vec{v}\right). \tag{3.4}$$
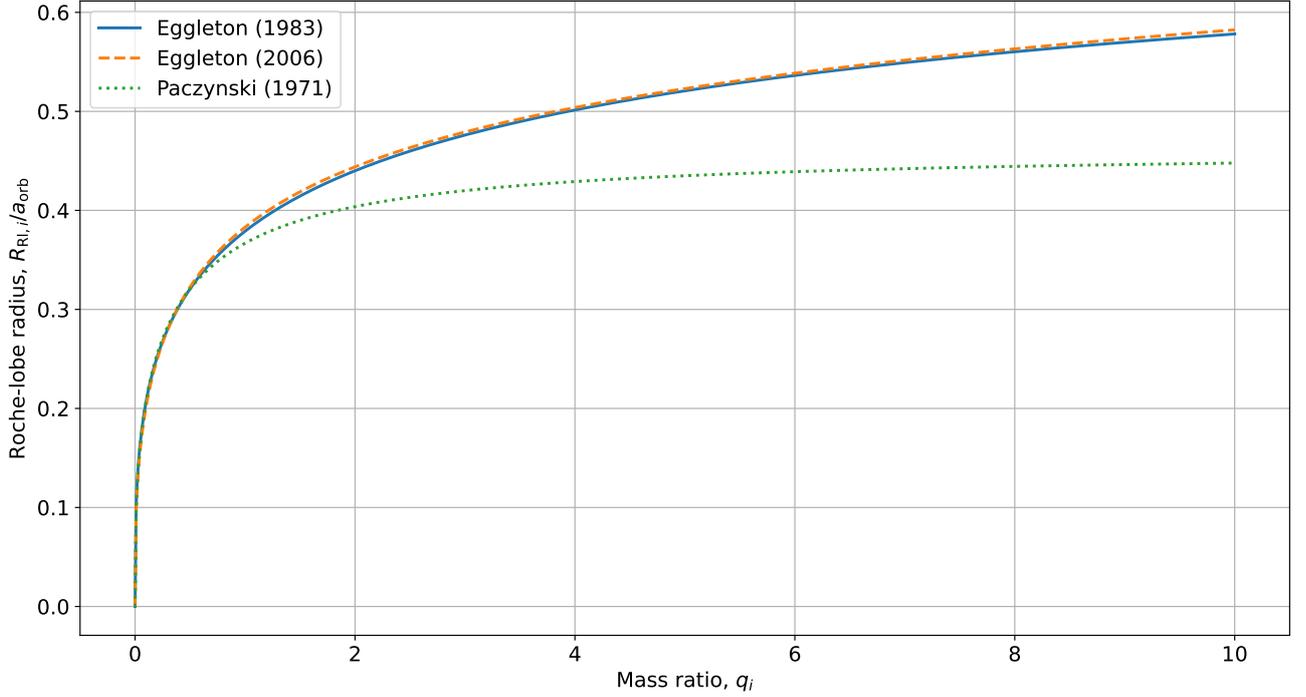
Figure 3.3: Fit of the Roche-lobe radius by Eggleton (1983) and its approximation by Eggleton (2006) (both in Eq. 3.6), compared to Paczyński (1971, see our Eq. 3.5).

3.1 Roche-lobe radius

An approximation for the Roche-lobe radius accurate within 2% for $0 < q_i < 0.8$ is given by Paczyński (1971):[2]

$$\frac{R_{\mathrm{Rl,i}}}{a} \approx \frac{2}{3^{4/3}} \left(\frac{M_i}{M_{\mathrm{T}}} \right)^{1/3} = \frac{2}{3^{4/3}} \left(\frac{q_i}{q_i + 1} \right)^{1/3}. \tag{3.5}$$

An approximation accurate (the first part of Eq. 3.6) within 1% for $0 < q_i < \infty$ was derived by Eggleton (1983) (see Fig. 3.3):

$$\frac{R_{\mathrm{Rl,i}}}{a} \approx \frac{0.49\, q_i^{2/3}}{0.6\, q_i^{2/3} + \ln\left(1 + q_i^{1/3}\right)} \approx \frac{0.44\, q_i^{0.33}}{(1 + q_i)^{0.2}}. \tag{3.6}$$

The last part is less accurate, but more convenient to work with (Eggleton, 2006, p. 111).

In fact, the approximations above provide the radius that a spherical star should have in order to have a volume that equals the droplet-shaped volume of its Roche lobe. This is useful for binary-evolution codes, where the stars are often one-dimensional (hence implicitly assumed to be spherically symmetric and therefore "single").

3.2 Roche-lobe overflow

If a star has a radius larger that its Roche-lobe radius, it is said to (over)fill its Roche lobe, and mass transfer from the Roche-lobe-filling star to its companion can occur through the first Lagrangian point L_1 (see Fig. 3.1). Section 7 is dedicated to mass transfer.

For a binary in which star i fills its Roche lobe (see Appendix A.7):

$$P_{\mathrm{orb}} \approx 0.35 \left(\frac{R_i^3}{M_i} \right)^{1/2} \left(\frac{2}{1 + q_i} \right)^{0.2} \mathrm{days}. \tag{3.7}$$

---

[2]Note that there is a typo in this equation in Paczyński (1967).

In general, for a Roche-lobe-filling star i

$$P_{\mathrm{orb}} \propto (\bar{\rho}_i)^{-1/2} \tag{3.8}$$

(see Appendix A.8).

Note that for a main-sequence star, roughly $R \propto M$ and hence $\bar{\rho} \propto M^{-2}$, so that lower-mass stars have *higher* densities and therefore shorter orbital periods when they are Roche-lobe filling and other circumstances are equal.

4 Orbital energy and angular momentum

4.1 Orbital energy

The orbital energy of a circular binary is given by:

$$E_{\mathrm{orb}} = E_{\mathrm{pot}} + E_{\mathrm{kin}} = -\frac{GM_1M_2}{a} + \frac{GM_1M_2}{2a} = -\frac{GM_1M_2}{2a}. \tag{4.1}$$

The "stellar unit" for gravitational energy is

$$\frac{GM_{\odot}^2}{R_{\odot}} \approx 3.79 \times 10^{41} \text{ J} \approx 3.79 \times 10^{48} \text{ erg}. \tag{4.2}$$

4.2 Orbital angular momentum

The orbital angular momentum (AM) of binary component i in a circular orbit (see Figure 2.1):[3]

$$J_i = |\vec{J_i}| = M_i |\vec{a}_i \times \vec{v}_i| = M_i a_i v_i = M_i a_i^2 \omega \; (= I_i \omega) = \frac{M_i M_{(3-i)}^2}{M_{\mathrm{T}}} \left(\frac{Ga}{M_{\mathrm{T}}} \right)^{1/2}, \tag{4.3}$$

where $I_i = M_i a_i^2$ is the *moment of inertia*, and $I_{\mathrm{orb}} = M_1 a_1^2 + M_2 a_2^2 = \mu a_{\mathrm{orb}}^2$. The total orbital angular momentum equals the sum of the angular momenta of the two stars (see Appendix A.10):

$$
\begin{aligned}
J_{\mathrm{orb}} &= J_1 + J_2 = \mu a^2 \omega \; (= I_{\mathrm{orb}} \omega) = \mu a^2 \frac{2\pi}{P} & (4.4) \\
&= M_1 M_2 \left(\frac{G^2}{M_{\mathrm{T}}} \frac{P}{2\pi} \right)^{1/3} & (4.5) \\
&= M_1 M_2 \left(\frac{Ga}{M_{\mathrm{T}}} \right)^{1/2} = \mu \sqrt{G M_{\mathrm{T}} a}. & (4.6)
\end{aligned}
$$

The "stellar unit" for angular momentum is

$$G^{1/2} M_{\odot}^{3/2} R_{\odot}^{1/2} \approx 6.04 \times 10^{44} \text{ J s} \approx 6.04 \times 10^{51} \text{ erg s}. \tag{4.7}$$

Inversely, the orbital period and separation can be computed from the angular momentum:

$$P = \left(\frac{J_{\mathrm{orb}}}{\mu} \right)^3 \frac{2\pi}{G^2 M_{\mathrm{T}}^2} = 2\pi \frac{M_{\mathrm{T}}}{G^2} \left(\frac{J_{\mathrm{orb}}}{M_1 M_2} \right)^3 ; \tag{4.8}$$

$$a = \frac{J_{\mathrm{orb}}^2}{\mu^2 G M_{\mathrm{T}}} = \left(\frac{J_{\mathrm{orb}}}{M_1 M_2} \right)^2 \frac{M_{\mathrm{T}}}{G}. \tag{4.9}$$

---

[3]Often, in particular in quantum mechanics, the symbol L is used to express *orbital* AM whereas J indicates the *total* AM (which might include the spin AM S of the bodies). In binary evolution, as in this document, this difference is often ignored and J is used throughout. In many cases, the spins of the stars in a binary may be ignored, although this is typically not the case when a star is filling its Roche lobe!

The orbital angular momentum for binary component i is given by:

$$J_i = J_{\mathrm{orb}} \frac{M_{(3-i)}}{M_{\mathrm{T}}} = \mu \frac{J_{\mathrm{orb}}}{M_i}, \tag{4.10}$$

so that

$$\frac{J_i}{J_{\mathrm{orb}}} = \frac{M_i\, a_i^2\, \omega}{\mu\, a^2\, \omega} = \frac{M_{(3-i)}}{M_{\mathrm{T}}}. \tag{4.11}$$

The specific orbital angular momentum for binary component i, *i.e.* the average amount of AM in a gram of stellar material, can be written as:

$$h_{\mathrm{i}} = \frac{J_{\mathrm{i}}}{M_{\mathrm{i}}} = a_i v_i = a_i^2 \omega = J_{\mathrm{orb}} \frac{M_{(3-i)}}{M_{\mathrm{i}}\, M_{\mathrm{T}}} = \mu \frac{J_{\mathrm{orb}}}{M_{\mathrm{i}}^2}. \tag{4.12}$$

Note that we have not considered the *spin* angular momenta of the stars here, which may be appreciable for large Roche-lobe-filling stars.

5 Orbital angular-momentum loss in detached binaries

A general equation for angular-momentum loss from a binary can be obtained by taking the logarithmic derivatives of Eqs. 4.5 and 4.6 (see Appendix A.1):

$$\frac{\dot{J}}{J} = \frac{\dot{M}_1}{M_1} + \frac{\dot{M}_2}{M_2} - \frac{1}{3}\frac{\dot{M}_{\mathrm{T}}}{M_{\mathrm{T}}} + \frac{1}{3}\frac{\dot{P}}{P}; \tag{5.1}$$

$$= \frac{\dot{M}_1}{M_1} + \frac{\dot{M}_2}{M_2} - \frac{1}{2}\frac{\dot{M}_{\mathrm{T}}}{M_{\mathrm{T}}} + \frac{1}{2}\frac{\dot{a}}{a}. \tag{5.2}$$

5.1 Stellar winds

Consider a detached binary with a fast $(v_{\mathrm{wind}} \gg v_{\mathrm{orb}})$, isotropic stellar wind from star 1 only. In that case $\dot{M}_{\mathrm{T}} = \dot{M}_1 \equiv \dot{M}$, $\dot{M}_2 = 0$ and $\dot{J} = \dot{J}_1$. Equation 5.2 then becomes

$$\frac{\dot{a}}{a} = 2\frac{\dot{J}}{J} - 2\frac{\dot{M}}{M_1} + \frac{\dot{M}}{M_{\mathrm{T}}}. \tag{5.3}$$

Each gram that is lost from the system carries the specific angular momentum of star 1, *i.e.* h_1 (Eq. 4.12), and the AM loss is related to the mass loss as: $\dot{J}_1 = h_1\, \dot{M}_1$, so that:

$$\left(\frac{\dot{J}}{J_{\mathrm{orb}}}\right)_{\mathrm{wind}} = \frac{M_2}{M_1}\frac{\dot{M}}{M_{\mathrm{T}}} = \frac{1}{q_1}\frac{\dot{M}}{M_{\mathrm{T}}}, \tag{5.4}$$

and Eq. 5.3 can be written as

$$\frac{\dot{a}}{a} = 2\left(\frac{\dot{J}}{J_{\mathrm{orb}}}\right)_{\mathrm{wind}} = -\frac{\dot{M}}{M_{\mathrm{T}}}. \tag{5.5}$$

See Appendix A.11 for a derivation of these equations.

Note that this result is *independent* of which star loses the mass and is generally applicable to wind mass loss. Hence

$$\frac{\dot{a}}{a} = -\frac{\dot{M}}{M_{\mathrm{T}}}; \quad a \propto M_{\mathrm{T}}^{-1}, \tag{5.6}$$

or, equivalently,

$$\frac{\dot{P}}{P} = -2\frac{\dot{M}}{M_{\mathrm{T}}}; \quad P_{\mathrm{orb}} \propto M_{\mathrm{T}}^{-2}. \tag{5.7}$$
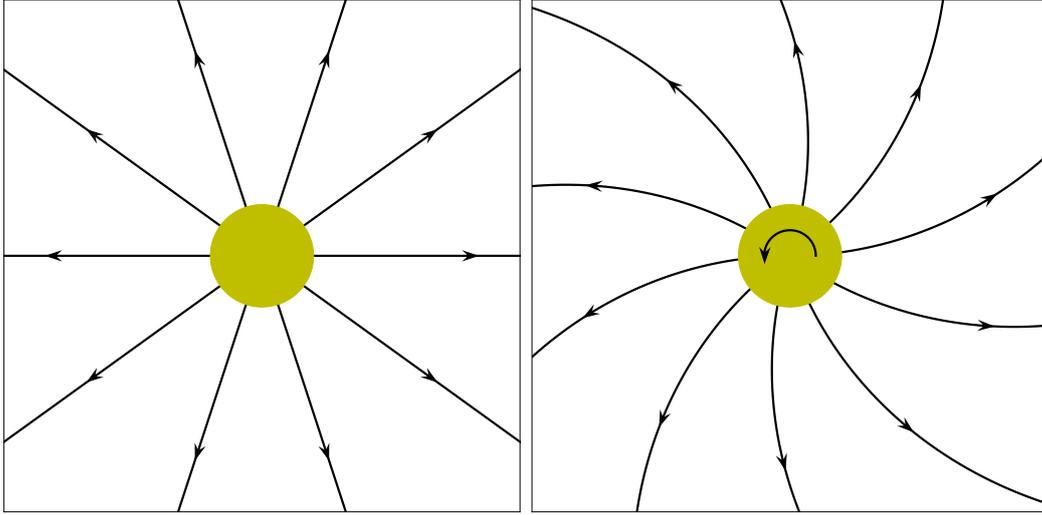
Figure 5.1: Illustration of magnetic braking. Left panel: the stellar wind of a non- or weakly magnetic star travels in straight trajectories and carries away the specific angular momentum from the surface of the star. Right panel: seen from the rest frame, the ionised wind of a rotating star with a strong magnetic field is forced to follow the magnetic-field lines and hence corotate with the star out to large distances. It thus follows curved trajectories and carries away much more angular momentum from the star once the wind decouples, braking the star's rotation much more efficiently.

5.2 Magnetic braking

Magnetic braking removes angular momentum from a rotating star with a magnetic field. If such a star is in a binary, and (close to) Roche-lobe filling, tidal effects may force the star to corotate with the orbit, essentially removing this angular momentum from the binary orbit. A prescription for the angular-momentum loss due to magnetic braking is given by *e.g.* Verbunt & Zwaan (1981):

$$\left(\frac{dJ}{dt}\right)_{\text{MB}} \approx -3.8 \times 10^{-30} \, M \, R^4 \, \omega^3 \, \text{dyn cm.} \tag{5.8}$$

For rapidly-rotating stars, it is assumed that the magnetic field strength may no longer increase with the rotational period of the star, "saturating" the magnetic braking. A prescription for saturated magnetic braking is given by *e.g.* Sills et al. (2000) (see van der Sluys et al., 2005, for a complete set of equations):

$$\left(\frac{dJ}{dt}\right)_{\text{MB}} = -K \left(\frac{R}{R_\odot}\right)^{1/2} \left(\frac{M}{M_\odot}\right)^{-1/2} \omega^3, \quad \omega \leq \omega_{\text{crit}} \tag{5.9}$$

$$= -K \left(\frac{R}{R_\odot}\right)^{1/2} \left(\frac{M}{M_\odot}\right)^{-1/2} \omega\omega_{\text{crit}}^2, \quad \omega > \omega_{\text{crit}} \tag{5.10}$$

5.3 Gravitational waves

Angular momentum lost due the emission of gravitational waves (GWs) for a binary in a *circular orbit* is given by:

$$\left(\frac{dJ}{dt}\right)_{\text{GW}} = -\frac{32}{5} \frac{G^{7/2}}{c^5} \frac{M_1^2 \, M_2^2 \, M_{\text{T}}^{1/2}}{a^{7/2}} \tag{5.11}$$

$$= -\frac{32}{5} \frac{G^{7/3}}{c^5} \left(\frac{M_1 \, M_2}{M_{\text{T}}^{1/3}}\right)^2 \left(\frac{2\pi}{P}\right)^{7/3} \tag{5.12}$$

$$= -\frac{32}{5} \frac{G^7}{c^5} \left(\frac{M_1 \, M_2}{M_{\text{T}}^{1/3}}\right)^9 J^{-7} \tag{5.13}$$

(Peters, 1964), where a power of the *chirp mass* can be recognised (see Eq. 2.6). This can be expressed as a logarithmic derivative as:

$$\left(\frac{\dot{J}}{J}\right)_{\text{GW}} = -\frac{32}{5}\frac{G^3}{c^5}\frac{M_1 M_2 M_{\text{T}}}{a^4} \tag{5.14}$$

$$= -\frac{32}{5}\frac{G^{5/3}}{c^5}\frac{M_1 M_2}{M_{\text{T}}^{1/3}}\left(\frac{2\pi}{P}\right)^{8/3} \tag{5.15}$$

$$= -\frac{32}{5}\frac{G^7}{c^5}\left(\frac{M_1 M_2}{M_{\text{T}}^{1/3}}\right)^9 J^{-8}. \tag{5.16}$$

The timescale for angular-momentum loss due to GWs is then:

$$\tau_{\text{GW}} \equiv \left|\frac{J}{\dot{J}}\right|_{\text{GW}} \approx 375\,\text{Gyr}\,\frac{(1+q)^2}{q}\left(\frac{M_{\text{T}}}{M_\odot}\right)^{-5/3}\left(\frac{P}{\text{day}}\right)^{8/3}, \tag{5.17}$$

which contains the *asymmetric mass ratio* (see Eq. 2.5). The time until contact or merger for a given detached binary is:

$$t_{\text{contact}} = \frac{\tau_{\text{GW}}}{8} = \frac{5}{256}\frac{c^5}{G^3}\frac{a^4}{M_1 M_2 M_{\text{T}}} \approx 150\,\text{Myr}\,\left(\frac{a_{\text{orb}}}{R_\odot}\right)^4\left(\frac{M_1}{M_\odot}\right)^{-1}\left(\frac{M_2}{M_\odot}\right)^{-1}\left(\frac{M_{\text{T}}}{M_\odot}\right)^{-1} \tag{5.18}$$

$$= \frac{5}{256}\frac{c^5}{G^{5/3}}\frac{M_{\text{T}}^{1/3}}{M_1 M_2}\left(\frac{P}{2\pi}\right)^{8/3} \approx 47.1\,\text{Gyr}\,\left(\frac{M_{\text{T}}}{M_\odot}\right)^{1/3}\left(\frac{M_1}{M_\odot}\right)^{-1}\left(\frac{M_2}{M_\odot}\right)^{-1}\left(\frac{P}{\text{day}}\right)^{8/3}. \tag{5.19}$$

See Appendix A.12 for a derivation of these equations.

6 Spin angular momentum

The spin angular momentum of a rotating body S is given by

$$S = I\,\omega = M\,k^2\,\omega, \tag{6.1}$$

where I is the moment of inertia, M the mass of the object, k its radius of gyration and ω the angular velocity of the rotating body (*e.g.* Wikipedia, 2021).

6.1 Black holes and neutron stars

In black holes and neutron stars, the spin is often indicated by a normalised dimensionless quantity

$$a_{\text{spin}} \equiv \frac{cS}{GM^2}, \tag{6.2}$$

where S is the spin angular momentum, M the mass and c and G are the speed of light and Newton's constant, respectively. The radius of the *event horizon* is given by

$$R_{\text{e}} = \frac{GM}{c^2}\left(1 + \sqrt{1 - a_{\text{spin}}^2}\right). \tag{6.3}$$

For a maximally spinning black hole, this gives $R_{\text{e}} = \frac{GM}{c^2}$, while for a non-spinning black hole it reduces to the Schwarzschild radius $R_{\text{e}} = R_{\text{s}} = \frac{2GM}{c^2}$.[4] Note that there are no real-valued solutions to Eq. 6.3 for $a_{\text{spin}} > 1$, in which case there is no horizon and we have a *naked singularity*.

---

[4]Note that black-hole physicists often use *geometrised* or *natural* units, using $c = G = 1$ (sometimes even $M = 1$). In this case, the Schwarzschild radius is given by $R_{\text{s}} = 2M$ for zero spin while $R_{\text{e}} = M$ for maximum spin, and the definition of spin becomes $a = \frac{S}{Mc} = S/M$ (since $c = 1$), with $0 \le a/M \le 1$.

The radius of a neutron star depends on its equation of state, which is uncertain, but is typically on the order of 10 km. For a hypothetical spherical neutron star with constant density ($I = \frac{2}{5}MR^2$) we find

$$a_{\rm spin} = \frac{4\pi c}{5G}\frac{R^2}{MP} \approx 0.58 \left(\frac{R}{12\,{\rm km}}\right)^2 \left(\frac{M}{1.4\,M_\odot}\right)^{-1} \left(\frac{P}{\rm ms}\right)^{-1}. \tag{6.4}$$

Realistic neutron stars rotate at breakup speed around $a_{\rm spin} \sim 0.7$ (Miller et al., 2011).

7 Stable mass transfer

7.1 Drives of mass transfer

Mass transfer between the donor star and the accretor can be driven by a number of processes. The mass-transfer rate can be estimated roughly from the timescale of the appropriate process τ:

$$\dot{M} \sim \frac{M_{\rm donor}}{\tau}. \tag{7.1}$$

Mass transfer can be driven by *intrinsic* changes, *i.e.* changes in the donor star (see Sect. 7.2):

- dynamical instability of the donor. $\dot{M}_{\rm dyn} \sim \frac{M_{\rm donor}}{\tau_{\rm dyn}}$ (see Sect.1.4.1);

- thermal evolution of the donor: $\dot{M}_{\rm th} \sim \frac{M_{\rm donor}}{\tau_{\rm th}}$ (see Sect.1.4.2);

- nuclear evolution of the donor: $\dot{M}_{\rm nuc} \sim \frac{M_{\rm donor}}{\tau_{\rm nuc}}$ (see Sect.1.4.3);

Mass transfer may also be driven by *extrinsic* changes, *i.e.* loss of angular momentum, *e.g.*:

- mass loss from the system (see Sects. 5.1, 7.4);

- gravitational waves (see Sect. 5.3);

- magnetic braking (see Sect. 5.2);

- tidal dissipation.

7.2 Stability of mass transfer

Once mass transfer (MT) commences, its stability depends on the response of the radius of the donor star and the response of the Roche-lobe radius to the mass loss of the donor and possible mass gain of the accretor. These responses are usually expressed using the logarithmic derivative and the Greek letter ζ defined as $R(M) \sim M^\zeta$:

$$\zeta \equiv \left(\frac{d\log R}{d\log M}\right) \tag{7.2}$$

(see *e.g.* Hjellming & Webbink, 1987; Soberman et al., 1997). In order for the mass transfer to be stable, the donor star must remain within its Roche lobe; hence the radius of the donor star must shrink more rapidly or expand less rapidly than the radius of the donor's Roche lobe during the MT:

$$\zeta_{\rm d} \geq \zeta_{\rm Rl}. \tag{7.3}$$

Note that for a higher value of ζ, the star's radius grows more rapidly that its Roche lobe upon mass *gain*. Hence, a donor star *shrinks* more rapidly upon mass *loss*. In other words, $d\log M$ is negative in such a case. In fact, violation of the inequality in Eq. 7.3 only indicates that the mass-transfer rate *increases*. If this is temporary, the mass transfer may stabilise after an initial increase in $\dot{M}$. If this is prolonged, mass transfer will become unstable.

In the range of stability of mass transfer, there are three regimes:

1. MT is thermally stable, and proceeds on the nuclear-evolution timescale;

2. MT is thermally unstable, but dynamically stable, and proceeds on the thermal timescale;

3. MT is dynamically unstable, and proceeds on the dynamical timescale (as a common envelope).

In order to determine on which timescale the mass transfer occurs, one will have test whether the MT will be thermally stable by comparing the *Kelvin-Helmholtz* mass-radius exponent $\zeta_{d,KH}$ to the Roche-lobe exponent ζ_{Rl}. For giants, a core-mass–radius relation is often assumed, which would yield the radius (almost) independent of the total mass and hence

$$\zeta_{d,KH} \sim 0. \tag{7.4}$$

If this test indicates thermally unstable MT, one will have to do a second test, comparing the *adiabatic* exponent $\zeta_{d,ad}$ to ζ_{Rl}.

The adiabatic response of a *giant* star's radius to mass loss, based on a polytrope with $n = 3/2$, is given to 1% accuracy by

$$\zeta_{ad} = \frac{2}{3}\frac{m_c}{1 - m_c} - \frac{1}{3}\frac{1 - m_c}{1 + 2m_c} - 0.03m_c + 0.2\frac{m_c}{1 + (1 - m_c)^{-6}}, \tag{7.5}$$

where $m_c = M_{He,d}/M_d$ is the mass fraction of the donor's helium core (Soberman et al., 1997).

The response of the donor's Roche-lobe radius to the mass transfer depends on the mass ratio of the binary $q \equiv M_d/M_a$ and the accretion efficiency $0 \leq \beta \leq 1$, defined as $\beta = 1$ for conservative (all mass lost from the donor is accreted by the secondary) and $\beta = 0$ as completely non-conservative MT:

$$
\begin{aligned}
\zeta_{Rl}(q,\beta) &= \frac{\partial \ln a}{\partial \ln M_d} + \frac{\partial \ln(R_{Rl}/a)}{\partial \ln q}\frac{\partial \ln q}{\partial \ln M_d} \\
&= \frac{2M_d^2 - 2M_a^2 - M_d M_a(1 - \beta)}{M_a(M_d + M_a)} + \left[\frac{2}{3} - \frac{q^{1/3}}{3}\frac{1.2\,q^{1/3} + 1/\left(1 + q^{1/3}\right)}{0.6\,q^{2/3} + \ln\left(1 + q^{1/3}\right)}\right]\left[1 + \beta\frac{M_d}{M_a}\right]. \tag{7.6}
\end{aligned}
$$

The second term in Eq. 7.6 comes from the approximation for the Roche-lobe radius by Eggleton (1983, see our Eq. 3.6). For a derivation, see Sect. 2.3 in Woods et al. (2012).

7.3 Stable, conservative mass transfer

If mass transfer (MT) from the donor star (with mass M_d) to the accretor (with mass M_a) is conservative, and ignoring stellar winds and other sources of angular-momentum loss, $\dot{M}_a = -\dot{M}_d$, $\dot{M}_T = 0$ and $\dot{J} = 0$. We then find from Eqs. 5.1 and 5.2:

$$\frac{\dot{P}}{P} = 3\dot{M}_d\left(\frac{M_d - M_a}{M_d M_a}\right) = 3\frac{\dot{M}_d}{M_d}(q - 1) \tag{7.7}$$

and

$$\frac{\dot{a}}{a} = 2\dot{M}_d\left(\frac{M_d - M_a}{M_d M_a}\right) = 2\frac{\dot{M}_d}{M_d}(q - 1) \tag{7.8}$$

(see Appendix A.13). Note that

- if $M_d > M_a$ and MT happens from star 1 to star 2, $\dot{M}_d < 0$, hence $\dot{a} < 0$ and the orbit shrinks;

- $\dot{a} = 0$ when $M_d = M_a$, hence the orbit starts expanding when the mass ratio flips.

The orbital evolution is then described by:

$$\frac{a}{a_{min}} = \left(\frac{M_T^2}{4M_d M_a}\right)^2, \tag{7.9}$$

where

$$a_{min} = \frac{16J^2}{GM_T^3} \tag{7.10}$$

(see Figure 7.1 and Appendix A.13).
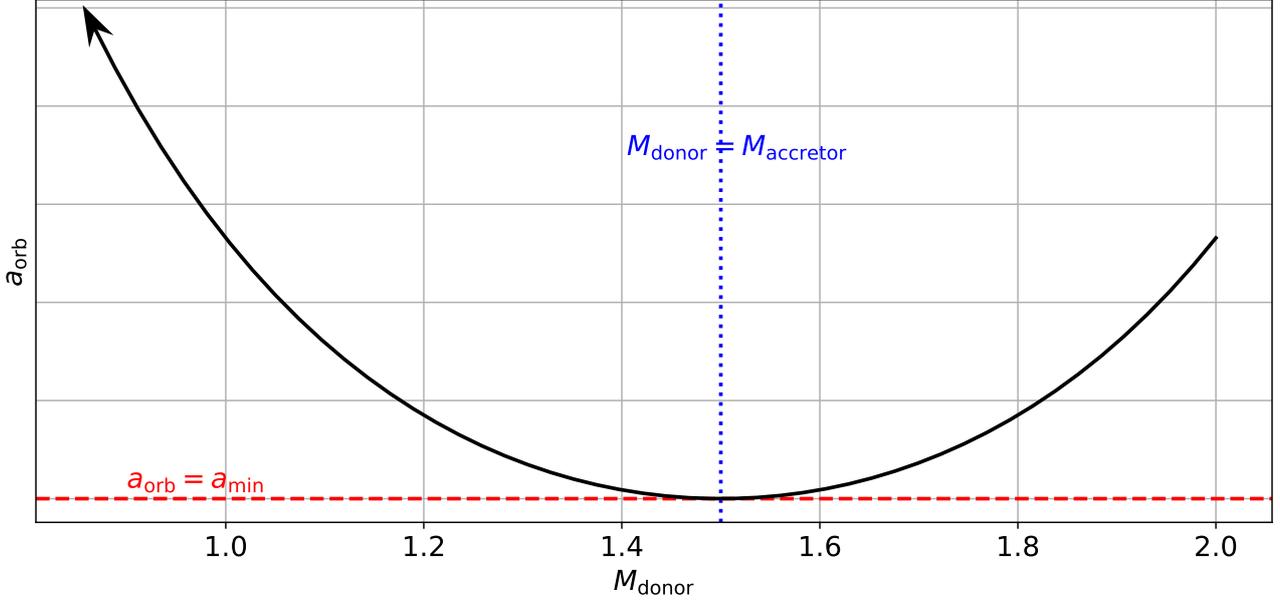
Figure 7.1: Schematic orbital evolution for conservative mass transfer according to Eq. 7.9. Note that the donor star is initially more massive than the accretor, and that the system evolves from right to left in this figure.

7.4 Stable, non-conservative mass transfer

Stable mass transfer is not necessarily conservative. Especially when mass-transfer rates are high, the accretor may not be able to accrete all the material lost by the donor. The material is often assumed to be transferred from the donor to the accretor first, after which only a fraction $\beta < 1$ may be accreted ($\dot{M}_a = -\beta \dot{M}_d$). The rest, $1 - \beta$, is assumed to be lost from the binary with a fraction α of the specific angular momentum of the *accretor*. The angular momentum lost from the system in this case can be derived from Equation 4.3:

$$\left(\frac{dJ}{dt}\right)_{\mathrm{MT}} = \alpha(1-\beta)\,a_a^2\,\omega\,\dot{M}_d \tag{7.11}$$

$$= \alpha(1-\beta)\,G^{2/3}\left(\frac{P}{2\pi}\right)^{1/3}\frac{M_d^2}{M_T^{4/3}}\dot{M}_d. \tag{7.12}$$

Written as a logarithmic derivative, this becomes

$$\left(\frac{\dot{J}}{J}\right)_{\mathrm{MT}} = \alpha(1-\beta)\frac{M_d}{M_a}\frac{\dot{M}_d}{M_T} = \alpha(1-\beta)\,q_d\,\frac{\dot{M}_d}{M_T}. \tag{7.13}$$

See Appendix A.14 for a derivation of this equation.

7.5 The Eddington limit

When a compact object (*e.g.* NS, BH) accretes matter, it radiates away energy produced from the infalling matter (*e.g.* through friction in the accretion disc). If this luminosity becomes sufficiently high, the radiation pressure may prevent further accretion. Hence, there is a maximum accretion rate for an accretor, known as the *Eddington limit*.

For simplicity, we assume that the accreted matter is a plasma and each "particle" has the mass of a *proton* m_p and the Thomson cross section of an *electron* $\sigma_T \approx 6.65 \times 10^{-29}\,\mathrm{m}^2$. Furthermore, if the momentum of a photon is given by $p = E/c$, then the momentum that can be transferred from the photons to the

infalling matter per unit of time is $\dot{p} = L/c$. If the luminosity force cancels out gravity on such a particle, then

$$F_{\mathrm{L}} = F_{\mathrm{g}} \quad \rightarrow \quad \frac{L}{c}\frac{\sigma_{\mathrm{T}}}{4\pi r^2} = \frac{G M_{\mathrm{a}} m_{\mathrm{p}}}{r^2}, \tag{7.14}$$

so that the *Eddington luminosity* (L_{edd}) can be defined as

$$L_{\mathrm{edd}} = \frac{4\pi c\, G\, m_{\mathrm{p}}}{\sigma_{\mathrm{T}}}\, M_{\mathrm{a}} \approx 3.3 \times 10^4 \left(\frac{M_{\mathrm{a}}}{M_{\odot}}\right) L_{\odot}. \tag{7.15}$$

The luminosity caused by the accretion comes from the stream of material falling into the gravitational potential well of the accretor with radius R_{a}

$$L_{\mathrm{acc}} = \frac{G M_{\mathrm{a}} \dot{M}}{R_{\mathrm{a}}}, \tag{7.16}$$

so that we can define the *Eddington accretion limit* ($\dot{M}_{\mathrm{edd}}$) as

$$\dot{M}_{\mathrm{edd}} = \frac{4\pi c\, m_{\mathrm{p}}}{\sigma_{\mathrm{T}}}\, R_{\mathrm{a}} \approx 1.5 \times 10^{-8} \left(\frac{R_{\mathrm{a}}}{10\,\mathrm{km}}\right) M_{\odot}\,\mathrm{yr}^{-1}. \tag{7.17}$$

8 Unstable mass transfer

8.1 Classical common envelope

A common envelope (CE) is used to explain many observed compact binaries (Paczynski, 1976). A CE is initiated when mass transfer is dynamically unstable and hence (the initial phase of) a CE takes place on the short dynamical timescale. The orbital change due to a classical common envelope is described by energy balance between the orbit and the binding energy of the donor's envelope:

$$E_{\mathrm{bind,env}} = \alpha_{\mathrm{CE}}\, \Delta E_{\mathrm{orb}} = \alpha_{\mathrm{CE}} \left[\frac{G M_{\mathrm{d,f}} M_{\mathrm{a}}}{2a_{\mathrm{f}}} - \frac{G M_{\mathrm{d,i}} M_{\mathrm{a}}}{2a_{\mathrm{i}}}\right], \tag{8.1}$$

where I used the labels 'd' and 'a' for the donor and "accretor", respectively, even though the latter does not accrete much (Webbink, 1984).

In many papers and especially population-synthesis codes, the envelope binding energy is approximated by

$$E_{\mathrm{bind,env}} \approx \frac{G M_{\mathrm{env}} M_*}{\lambda_{\mathrm{env}} R_*}, \tag{8.2}$$

where λ_{env} is the *envelope structure parameter*, often assumed to be constant (*e.g.* $\lambda_{\mathrm{env}} = 0.5$). However, see Dewi & Tauris (2000); Tauris & Dewi (2001); van der Sluys et al. (2006, 2010) on values for λ_{env}, and Loveridge et al. (2010) on how to approximate $E_{\mathrm{bind,env}}$ (so that you no longer need λ_{env}).[5]

Still, much of the uncertainty in $E_{\mathrm{bind,env}}$ comes from the discussion of which energy sources should be included (in particular, can the recombination energy actually be used to expel the envelope), and, for massive stars ($M \gtrsim 5-8\,M_{\odot}$), from the uncertainty of which fraction of the star is left after the CE (*i.e.*, the definition of the core mass).

8.2 Envelope ejection based on AM conservation

Nelemans et al. (2000) showed that a combination of stable mass transfer and a classical CE cannot explain observed double white dwarfs (DWDs). They suggest a mode of envelope ejection (EE) where angular-momentum, rather than energy, balance is important:

$$\frac{J_{\mathrm{f}} - J_{\mathrm{i}}}{J_{\mathrm{i}}} = \gamma \frac{M_{\mathrm{1f}} - M_{\mathrm{1i}}}{M_{\mathrm{tot,i}}}, \tag{8.3}$$

---

[5]Their Fig. 7 shows that λ_{env} varies very differently with radius for stars with different masses (increasing, decreasing, or both) and that λ_{env} can take any value between 0.1 and 1.9.

where γ describes how many times the specific angular momentum of the *system* is carried away by the mass loss. Nelemans et al. (2000, 2001); Nelemans & Tout (2005) show that this works well for observed (populations of) DWDs for $\gamma \approx 1.5 - 1.75$. However, a clear physical picture of why this works and why γ should have these or any other values is currently lacking.

van der Sluys et al. (2006) used this idea and designed similar prescriptions for an envelope ejection with the specific angular momentum of the *donor* (γ_d, *e.g.* a strong stellar wind) and *accretor* (γ_a, isotropic wind from the accretor) respectively:

$$\frac{J_f - J_i}{J_i} = \gamma_d \frac{M_{1f} - M_{1i}}{M_{tot,f}} \frac{M_{2i}}{M_{1i}}; \tag{8.4}$$

$$\frac{J_f - J_i}{J_i} = \gamma_a \left[\frac{M_{tot,i}}{M_{tot,f}} \exp\left(\frac{M_{1f} - M_{1i}}{M_2} \right) - 1 \right]. \tag{8.5}$$

They show that a γ_d-EE for the formation of the first WD followed by a γ_a-EE for the formation of the second WD explains observed values of P, q and the difference in cooling age for DWDs well, for $\gamma_d, \gamma_a \approx 1.0$.

The γ-EE scenarios do not have to occur on the dynamical timescale, but must happen on a timescale that is short compared to the nuclear-evolution timescale (since the companion does not accrete, and the donor's core mass does not grow).

8.3 The Darwin instability

Apart from Roche-lobe overflow, a common envelope may be also initiated by what is known as the *Darwin instability* (Darwin, 1879). All three of the conditions below must be fulfilled in order for his instability to occur:

1. the spin angular momentum of one of the binary components exceeds $\frac{1}{3} J_{orb}$,

2. that star is tidally locked to the orbit, and

3. that star is expanding (due to evolution).

In this case, a stable binary orbit is no longer possible, and the two stars are bound to plunge into each other. When the star expands, it will slow its rotation. However, the tidal forces will spin it up again by extracting angular momentum from the orbit, so that the star will remain tidally locked to the orbit. When the orbit loses angular momentum, it will shrink and hence increase its orbital frequency. As a consequence, the star needs even more angular momentum from the orbit to keep pace, *et cetera*. This will result in an "angular-momentum catastrophe", an orbital spiral-in and a common envelope.

See Appendix A.15 for a derivation of the Darwin instability.

Appendices

A Derivation of basic equations

A.1 Logarithmic derivatives

Logarithmic derivatives, as used in *e.g.* Section 5, are useful when dealing with power laws of the form $x \equiv a\,y^b$. For such functions,

$$\frac{\dot{x}}{x} \;=\; \frac{b\,a\,y^{b-1}\,\dot{y}}{a\,y^b} \;=\; b\,\frac{\dot{y}}{y}, \tag{A.1}$$

where $\dot{x}$ denotes the (time) derivative of x.

This is called the *logarithmic* derivative, since one in fact takes the derivative of $\ln x$:

$$\frac{d\ln x}{dt} = \frac{1}{x}\frac{dx}{dt} = \frac{\dot{x}}{x}.$$

It is useful, because for functions that the product of a number of powers, one can "compute" derivatives without any calculation, simply by ignoring constant factors (the a above), replacing multiplication and division with addition and subtraction, and changing the powers into factors (b in this example). Conversely, the result can be quickly interpreted as a power law (here we can conclude that $x \propto y^b$).

A.2 Centre of mass

The position $\vec{R}$ of the centre of mass of N of particles is defined as the weighted mean position of all particles:

$$\vec{R} \equiv \frac{1}{M_{\rm T}} \sum_{i=1}^{N} m_i \vec{r}_i, \tag{A.2}$$

where m_i and $\vec{r}_i$ are the masses and positions of the individual particles and $M_{\rm T}$ is their total mass. For two stars in a binary with masses M_1 and M_2, positions $\vec{r}_1$ and $\vec{r}_2$ and orbital separation a, this reduces to

$$\vec{R} = \frac{M_1\vec{r}_1 + M_2\vec{r}_2}{M_{\rm T}}, \tag{A.3}$$

so that

$$M_{\rm T}\vec{R} = M_1\vec{r}_1 + M_2\vec{r}_2. \tag{A.4}$$

When we position star 1 in the origin of our coordinate system, $|\vec{r}_1| = 0$ and $|\vec{r}_2| = a$, and, since this is the definition of a_1 (see Fig. 2.1 on page 7), $|\vec{R}| = a_1$, so that Eq. A.4 reduces to

$$M_{\rm T}a_1 = M_2 a \;\rightarrow\; \frac{M_{\rm T}}{a} = \frac{M_2}{a_1}. \tag{A.5}$$

If instead we put the origin in the centre of mass, so that $|\vec{a}_i| = a_i$ and $R = 0$ (see Fig. 2.1 on page 7), we find that Eq. A.4 becomes

$$M_1\vec{a}_1 = -M_2\vec{a}_2 \;\rightarrow\; M_1 a_1 = M_2 a_2 \;\rightarrow\; \frac{M_1}{a_2} = \frac{M_2}{a_1} = \frac{M_{\rm T}}{a}, \tag{A.6}$$

where the last equality is copied from Eq. A.5. This yields Equation 2.9 (and 2.8) in Section 2.3.

Using Equation 2.8 and the definition of the reduced mass in Eq. 2.3, we find that

$$M_1 a_1 = M_1 \frac{M_2}{M_{\rm T}} a \equiv \mu a, \tag{A.7}$$

and the same for $M_2 a_2$, which results in Equation 2.10.
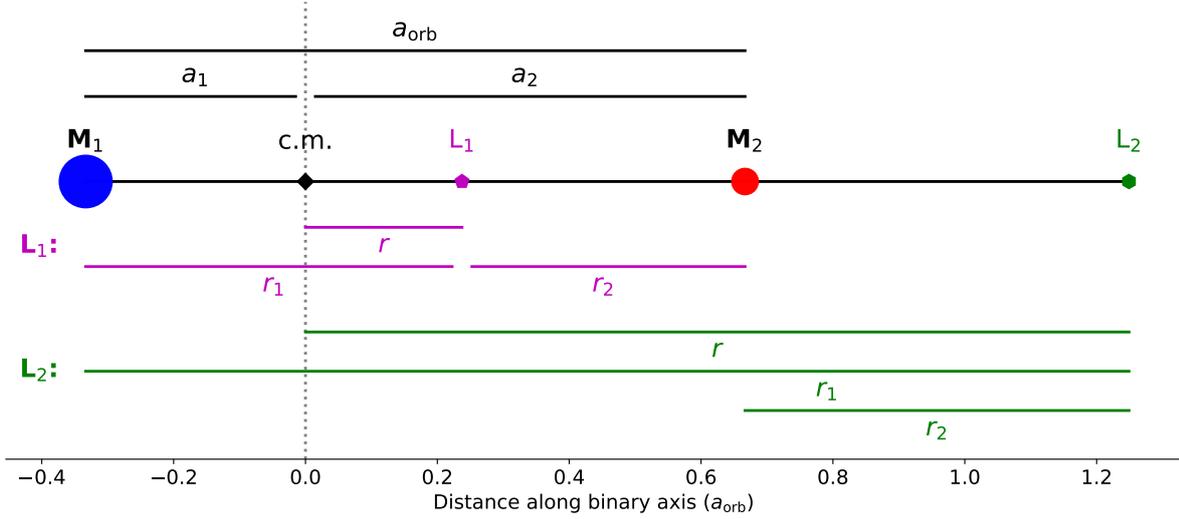
Figure A.1: Schematic one-dimensional geometry of a binary with component masses $M_1 = 2\,M_2$, and orbital separation a_{orb}, along the binary axis. The distances a_1, a_2, are from the binary members to the centre of mass (c.m.), which is also the rotation axis of the binary. The distances denoted by r and r_i show the distances to the first (L_1, in magenta) and second (L_2, in green) Lagrangian points in the Roche potential.

A.3 Kepler's law for a circular orbit

For a circular orbit the gravity between the two components must compensate the centrifugal force at all times. For star 1, this implies

$$\frac{GM_1M_2}{a^2} = \frac{M_1 v_{\text{orb},1}^2}{a_1} = \frac{M_1}{a_1}\left(\frac{2\pi a_1}{P_{\text{orb}}}\right)^2 = M_1 a_1\left(\frac{2\pi}{P_{\text{orb}}}\right)^2 = M_1\frac{M_2}{M_{\text{T}}}a\left(\frac{2\pi}{P_{\text{orb}}}\right)^2, \tag{A.8}$$

where G is Newton's gravitational constant, $v_{\text{orb},1} = \frac{2\pi a_1}{P}$ is the (constant) orbital velocity and I used Eq. 2.8 to eliminate a_1 in the last step. This gives us

$$\left(\frac{2\pi}{P_{\text{orb}}}\right)^2 = \frac{GM_1M_2}{a^2}\frac{M_{\text{T}}}{M_1M_2a} = \frac{GM_{\text{T}}}{a^3} = \omega^2, \tag{A.9}$$

which is Eq. 2.12. In the last step, I used the definition of the angular velocity $\vec{\omega} = \frac{\vec{r}\times\vec{v}}{r^2}$, so that $\omega \equiv |\vec{\omega}| = \frac{v}{r} = \frac{1}{r}\frac{2\pi r}{P}$ (for a circular orbit) $= \frac{2\pi}{P} = 2\pi f$. I would of course have arrived at the same result when starting from star 2.

A.4 The centrifugal potential

While the gravitational potential in Equation 3.1 on page 8 will be familiar to the reader, the centrifugal contribution in the last term may be less so. It can be made plausible (for a circular orbit) by realising that for a test mass m, $\dfrac{\vec{F}_{\text{centr}}}{m} \equiv -\nabla\Phi_{\text{centr}}$, so that

$$\Phi_{\text{centr}} = -\frac{1}{m}\int_0^r \vec{F}_{\text{centr}}\cdot d\vec{r} = -\frac{1}{m}\int_0^r -m\,\vec{\omega}\times(\vec{\omega}\times\vec{r})\cdot d\vec{r} = -\int_0^r \omega^2 r\,dr = -\frac{1}{2}\omega^2 r^2. \tag{A.10}$$

Note that Eq. A.10, r is the distance to the centre of mass of the binary. This result is consistent with a more detailed derivation which yields the $\Phi_{\text{centr}} = -\dfrac{1}{2}(\vec{\omega}\times\vec{r})^2$ in Eq. 3.1.

A.5 Lagrangian points in the Roche potential

The Lagrangian points or stationary points are defined by the fact that the net acceleration (or force on a test particle) equals zero, so that the Roche potential has a (local) minimum, maximum or saddle point.

22

This is equivalent to finding roots for the gradient of the Roche potential. We are here mostly interested in the location of L_1, through which mass can flow from one star to the other, and L_2 where mass can leave the binary system if both members fill their Roche lobes. Both of these Lagrangian points lie on the main axis of the binary, that connects the two stars.

We can therefore use Equation 3.1, and use Figure A.1 to reduce it to a one-dimensional problem for the simpified case of a circular orbit. We will define $r \equiv |\vec{r}|$ as the distance between the centre of mass and the Lagrangian point and $r_i \equiv |\vec{r} - \vec{r_i}|$ as the distance between star i and the Lagrangian point (not that the index i refers to the *star*, not the Lagrangian point!). Assuming a circular orbit, we can the write

$$(\vec{\omega} \times \vec{r})^2 = \omega^2 r^2 = \frac{GM_T}{a^3} r^2 \tag{A.11}$$

(see Eq. 2.12) and thus

$$\Phi_{\text{Roche}} = -\frac{GM_1}{r_1} - \frac{GM_2}{r_2} - \frac{1}{2}\frac{GM_T}{a^3}r^2 \;\propto\; \frac{M_1}{r_1} + \frac{M_2}{r_2} + \frac{M_T}{2a^3}r^2. \tag{A.12}$$

We do not have to worry here about the sign, since we will compute the gradient and equate it to zero. We can remove two out of r, r_1, r_2 by substitution. Experience teaches us that removing r and r_1 in favour of r_2 yields the easiest excercise and the simplest results. The substitution is different for L_1 than for L_2.

Using Figure A.1, we find that for L_1, we can substitute $r = a_2 - r_2$ and $r_1 = a - r_2$, and thus write

$$(-)\nabla\Phi_{\text{Roche}} = \nabla\left[\frac{M_1}{a - r_2} + \frac{M_2}{r_2} + \frac{M_T}{2a^3}(a_2 - r_2)^2\right] = \frac{M_1}{(a - r_2)^2} - \frac{M_2}{r_2^2} - \frac{M_T}{a^3}(a_2 - r_2) = 0. \tag{A.13}$$

Similarly, for L_2 we can write $r = a_2 + r_2$ and $r_1 = a + r_2$, and hence

$$(-)\nabla\Phi_{\text{Roche}} = \nabla\left[\frac{M_1}{a + r_2} + \frac{M_2}{r_2} + \frac{M_T}{2a^3}(a_2 + r_2)^2\right] = -\frac{M_1}{(a + r_2)^2} - \frac{M_2}{r_2^2} + \frac{M_T}{a^3}(a_2 + r_2) = 0. \tag{A.14}$$

We can use *e.g.* the Newton-Raphson method to find a numerical solution for r_2 for these two equaitions, and hence the distance between the Lagrangian point under consideration and star 2. Figure A.1 shows that the location of the L_1 point is then given by $r = a_2 - r_2$, since it lies "in front" of star 2 (as seen from the centre of mass), whereas for L_2, $r = a_2 + r_2$, as it lies "behind" that star.

A.6 Scale and shape of the Roche potential

As indicated in Equation 3.3, the Roche potential from Eq. 3.1 can be written as a *scale factor*, which depends on a and M_T, and a more complex function that describes the *shape* of the potential. We can achieve this by making the masses dimensionless through division by M_T, making the distances dimensionless through division by a and applying Kepler's law to substitute ω for M_T and a. We then find

$$\begin{aligned}
\Phi_{\text{Roche}}(r) &= -\frac{GM_1}{r_1} - \frac{GM_2}{r_2} - \frac{\omega^2 r^2}{2} = -\frac{GM_1}{r_1} - \frac{GM_2}{r_2} - \frac{GM}{a^3}\frac{r^2}{2} \\
&= -\frac{GM_T}{a}\left[\frac{M_1/M_T}{r_1/a} + \frac{M_2/M_T}{r_2/a} + \frac{(r/a)^2}{2}\right] \\
&= -\frac{GM_T}{a}\left[\frac{q_1}{q_1 + 1}\left(\frac{r_1}{a}\right)^{-1} + \frac{1}{q_1 + 1}\left(\frac{r_2}{a}\right)^{-1} + \frac{1}{2}\left(\frac{r}{a}\right)^2\right]. \tag{A.15}
\end{aligned}$$

Note that here r_1 and r_2 are the distances to the two stars and r is the distance to the centre of mass.

A.7 Period for a Roche-lobe-filling star

Equation 3.7 for the orbital period of a Roche-lobe-filling star can be derived from the approximation in Eq. 3.6:[6]

$$\frac{R_i}{a} \approx \frac{R_{\mathrm{Rl,i}}}{a} \approx 0.44 \frac{q_i^{0.33}}{(1+q_i)^{0.2}}, \quad \rightarrow \quad a^{3/2} \approx \left(\frac{R_i}{0.44}\right)^{3/2} \frac{(1+q_i)^{0.3}}{q_i^{0.5}}. \tag{A.16}$$

This fits surprisingly well into Kepler's law:

$$
\begin{aligned}
P_{\mathrm{orb}} &= \frac{2\pi}{\sqrt{GM_{\mathrm{T}}}} a^{3/2} \approx \frac{2\pi}{\sqrt{GM_{\mathrm{T}}}} \left(\frac{R_i}{0.44}\right)^{3/2} \frac{(1+q_i)^{0.3}}{q_i^{0.5}} = \frac{2\pi}{\sqrt{0.44^3\,G}} R_i^{3/2} \frac{(1+q_i)^{0.3}}{(q_i\,M_{\mathrm{T}})^{0.5}} \\
&= \frac{2\pi}{\sqrt{0.44^3\,G}} \frac{R_i^{3/2}}{M_i^{1/2}} \left(\frac{1}{q_i+1}\right)^{0.2} = 2\pi \left(\frac{R_\odot^3}{0.44^3\,GM_\odot}\right)^{1/2} \left(\frac{R_i}{R_\odot}\right)^{3/2} \left(\frac{M_i}{M_\odot}\right)^{-1/2} \left(\frac{1}{q_i+1}\right)^{0.2} \\
&\approx 0.39 \left(\frac{R_i}{R_\odot}\right)^{3/2} \left(\frac{M_i}{M_\odot}\right)^{-1/2} \left(\frac{1}{q_i+1}\right)^{0.2} \text{ days.}
\end{aligned}
\tag{A.17}
$$

This can be written as

$$P_{\mathrm{orb}} \approx 0.35 \left(\frac{R_i}{R_\odot}\right)^{3/2} \left(\frac{M_i}{M_\odot}\right)^{-1/2} \left(\frac{2}{q_i+1}\right)^{0.2} \text{ days,} \tag{A.18}$$

where I transferred the value of $2^{-0.2}$ to the constant in front to make $R_i = M_i = q_i = 1$ yield 0.35 days. Note that R_i and M_i are here expressed in cgs or SI units, whereas in Eq. 3.7 they are in solar units.

A.8 Period vs. density for a Roche-lobe-filling star

We can derive a relation between the orbital period and the mean density of the Roche-lobe filling star from Eq. 3.5 and Kepler's law:

$$R_i \approx R_{\mathrm{Rl,i}} \propto M_i^{1/3} \frac{a}{M_{\mathrm{T}}^{1/3}} \propto M_i^{1/3} P_{\mathrm{orb}}^{2/3}. \tag{A.19}$$

Hence,

$$P_{\mathrm{orb}} \propto \frac{R_i^{3/2}}{M_i^{1/2}} \propto \bar{\rho}_i^{-1/2}, \tag{A.20}$$

which is identical to Equation 3.8.

A.9 Orbital energy for a circular orbit

The orbital energy of a binary consists of the gravitational energy of the two masses and the two kinetical energies of the two stars. For a circular orbit, we can find the kinetic energy of star 1 from the fact that the gravity between the two components must compensate the centrifugal force at all times:

$$\frac{M_1 v_{\mathrm{orb,1}}^2}{a_1} = \frac{GM_1 M_2}{a^2}, \tag{A.21}$$

so that

$$E_{\mathrm{kin,1}} = \frac{M_1 v_{\mathrm{orb,1}}^2}{2} = \frac{GM_1 M_2}{a^2} \frac{a_1}{2} = \frac{GM_1 M_2}{2a^2} \frac{M_2}{M_{\mathrm{T}}} a = \frac{GM_1 M_2}{2M_{\mathrm{T}} a} M_2, \tag{A.22}$$

where I used Eq. 2.8 to eliminate a_1. Analogously, we find for star 2:

$$E_{\mathrm{kin,2}} = \frac{GM_1 M_2}{2M_{\mathrm{T}} a} M_1. \tag{A.23}$$

---

[6]I will use the original value 0.44224 from Eggleton (2006) in my actual calculations of the final constant.

Then the total orbital energy can be written as

$$E_{\mathrm{orb}} = E_{\mathrm{grav}} + E_{\mathrm{kin},1} + E_{\mathrm{kin},2} = \frac{-GM_1M_2}{a} + \frac{GM_1M_2}{2M_{\mathrm{T}}a}(M_2 + M_1) \tag{A.24}$$

$$= \frac{-GM_1M_2}{a} + \frac{GM_1M_2}{2a} = \frac{-GM_1M_2}{2a}. \tag{A.25}$$

A.10   Orbital angular momentum

Expressions for the orbital angular momentum of a binary can be derived from the general definition of the angular momentum:

$$J = J_1 + J_2 = \left[M_1 a_1^2 + M_2 a_2^2\right]\omega \;=\; \left[M_1\left(\frac{M_2}{M_{\mathrm{T}}}a\right)^2 + M_2\left(\frac{M_1}{M_{\mathrm{T}}}a\right)^2\right]\omega$$

$$= \frac{M_1M_2}{M_{\mathrm{T}}}\,a^2\omega \;=\; \mu a^2\omega, \tag{A.26}$$

in which we recognise Equation 4.4. When we apply Kepler's law to substitute ω, we find

$$J \;=\; \frac{M_1M_2}{M_{\mathrm{T}}}\,a^2\omega \;=\; \frac{M_1M_2}{M_{\mathrm{T}}}\,a^2\sqrt{\frac{GM_{\mathrm{T}}}{a^3}} \;=\; M_1M_2\sqrt{\frac{Ga}{M_{\mathrm{T}}}}, \tag{A.27}$$

identical to Eq. 4.6.

A.11   Stellar winds

The orbital angular-momentum loss due to stellar winds can be derived from Equations 5.3 and 4.12. Using the subscripts 'd' and 'a' to denote the donor star and the accretor respectively, we can write

$$\left(\frac{\dot{J}}{J_{\mathrm{orb}}}\right)_{\mathrm{wind}} \;=\; \frac{h_{\mathrm{d}}\dot{M}}{J_{\mathrm{orb}}} \;=\; \frac{J_{\mathrm{orb}}M_{\mathrm{a}}}{M_{\mathrm{d}}M_{\mathrm{T}}}\frac{\dot{M}}{J_{\mathrm{orb}}} \;=\; \frac{M_{\mathrm{a}}}{M_{\mathrm{d}}}\frac{\dot{M}}{M_{\mathrm{T}}} \;=\; \frac{1}{q_{\mathrm{d}}}\frac{\dot{M}}{M_{\mathrm{T}}}, \tag{A.28}$$

which yields Equation 5.4. We can then reuse Eq. 5.3 to find

$$\frac{\dot{a}}{a} = 2\left(\frac{\dot{J}}{J_{\mathrm{orb}}}\right)_{\mathrm{wind}} - 2\frac{\dot{M}}{M_{\mathrm{d}}} + \frac{\dot{M}}{M_{\mathrm{T}}} \;=\; \frac{2M_{\mathrm{a}}}{M_{\mathrm{d}}}\frac{\dot{M}}{M_{\mathrm{T}}} - \frac{2\dot{M}}{M_{\mathrm{d}}}\frac{M_{\mathrm{T}}}{M_{\mathrm{T}}} + \frac{\dot{M}}{M_{\mathrm{T}}}\frac{M_{\mathrm{d}}}{M_{\mathrm{d}}}$$

$$= \frac{\dot{M}}{M_{\mathrm{T}}}\frac{2M_{\mathrm{a}} - 2M_{\mathrm{T}} + M_{\mathrm{d}}}{M_{\mathrm{d}}} \;=\; \frac{\dot{M}}{M_{\mathrm{T}}}\frac{-M_{\mathrm{d}}}{M_{\mathrm{d}}} \;=\; -\frac{\dot{M}}{M_{\mathrm{T}}}, \tag{A.29}$$

which is identical to Eq. 5.5.

A.12   Gravitational waves

Expressions for the orbital angular-momentum loss due to the radiation of gravitational waves can be written as the logarithmic derivatives in Equations 5.14 and 5.15 by dividing Eqs. 5.11 and 5.12 by J_{orb} from Equations 4.6 and 4.5, respectively, where in the latter we need to apply Kepler's law from Eq. 2.13 to remove the orbital separation from the equation. Equation 5.16 can simply be found by dividing Eq. 5.13 by the variable J.

The time until contact can be found from Eq. 5.13 by noting that the latter equation can be integrated as

$$\int_{J_0}^{0} dJ\,J^7 = \int_{0}^{t_{\mathrm{contact}}} -\frac{32}{5}\frac{G^7}{c^5}\left(\frac{M_1\,M_2}{M_{\mathrm{T}}^{1/3}}\right)^9 dt, \tag{A.30}$$

so that

$$-\frac{J_0^8}{8} = -\frac{32}{5}\frac{G^7}{c^5}\left(\frac{M_1\,M_2}{M_{\mathrm{T}}^{1/3}}\right)^9 t_{\mathrm{contact}}. \tag{A.31}$$

When we compare this result to Eqs. 5.16 and 5.17, we find Equations 5.18 and 5.19.

A.13 Conservative mass transfer

If mass transfer in a binary is conservative, $\dot{M}_T = 0$, $\dot{M}_2 = -\dot{M}_1$ and $\dot{J} = 0$, so that Equation 5.2 becomes

$$\frac{\dot{J}}{J} = \frac{\dot{M}_1}{M_1} - \frac{\dot{M}_1}{M_2} + \frac{1}{2}\frac{\dot{a}}{a} = 0, \tag{A.32}$$

and

$$\frac{\dot{a}}{a} = 2\dot{M}_1\frac{M_1 - M_2}{M_1 M_2} = \frac{\dot{M}_1}{M_1}(q_1 - 1), \tag{A.33}$$

i.e. providing Eq. 7.8. Equation 7.7 can be derived analogously.

Equation 7.9 can be derived from Eq. 4.6, when considering that J_{orb} is constant and hence should always have the same value as for the case where $M_1 = M_2 = \frac{M_T}{2}$ where $a_{orb} = a_{min}$, so that

$$J_{orb} = \left(\frac{M_T}{2}\right)^2\left(\frac{Ga_{min}}{M_T}\right)^{1/2} = \frac{M_T^2}{4}\left(\frac{Ga_{min}}{M_T}\right)^{1/2}. \tag{A.34}$$

From this and again Equation 4.6 itself we then find

$$\frac{a}{a_{min}} = \left(\frac{J^2}{G}\frac{M_T}{M_1 M_2}\right)\left(\frac{16J^2}{GM_T^3}\right)^{-1} = \left(\frac{M_T^2}{4M_1 M_2}\right)^2. \tag{A.35}$$

A.14 Stable, non-conservative mass transfer

Consider the case where the donor star transfers mass at a rate $\dot{M}$ to the accretor, which accretes $-\beta\dot{M}$. The rest, $(1 - \beta)\dot{M}$, is lost from the binary with α times the specific angular momentum of the *accretor*, h_a. Then, the angular-momentum loss from the binary is given by the derivative of Equation 4.3 for the accreting star:

$$\dot{J}_a = \alpha(1 - \beta)\dot{M}a_a^2\omega = \alpha(1 - \beta)\dot{M}\left(\frac{M_d}{M_T}a\right)^2\omega, \tag{A.36}$$

where I used Eq. 2.8 to substitute a_a. According to Equation 4.4, the orbital angular momentum can be written as

$$J_{orb} = \mu a^2\omega = \frac{M_d M_a}{M_T}a^2\omega. \tag{A.37}$$

The logarithmic derivative for angular-momentum loss due to stable, non-conservative mass transfer can then be found by dividing Eq. A.36 by Eq. A.37:

$$\left(\frac{\dot{J}}{J}\right)_{MT} \equiv \frac{\dot{J}_d}{J_{orb}} = \frac{\alpha(1 - \beta)\dot{M}\frac{M_d^2}{M_T^2}a^2\omega}{\frac{M_d M_a}{M_T}a^2\omega} = \alpha(1 - \beta)\frac{M_d}{M_a}\frac{\dot{M}_d}{M_T} = \alpha(1 - \beta)q_d\frac{\dot{M}_d}{M_T}, \tag{A.38}$$

which is indeed identical to Equation 7.13.

A.15 The Darwin instability

The Darwin instability described in Section 8.3 can be derived by assuming that the angular momentum of the secondary star is negligible, thus writing the total angular momentum of the system as the sum of that of the orbit and that of (what is to become) the donor star using Equations 4.6 and 6.1:

$$J = J_{orb} + J_d = M_d M_a\left(\frac{Ga}{M_T}\right)^{1/2} + M_d\, k_d^2\,\omega = \frac{M_d M_a}{M_T}\frac{G^{2/3}}{\omega^{1/3}} + M_d\, k_d^2\,\omega. \tag{A.39}$$

We can then find a minimum in J as a function of ω by solving

$$\frac{dJ}{d\omega} = M_d\, k_d^2 - \frac{1}{3}\frac{G^{2/3}M_d M_a}{M_T}\omega^{-4/3} = 0. \tag{A.40}$$

Multiplying both sides with ω yields

$$M_\mathrm{d}\,k_\mathrm{d}^2\,\omega \;=\; \frac{1}{3}\frac{M_\mathrm{d}M_\mathrm{a}}{M_\mathrm{T}}\frac{G^{2/3}}{\omega^{1/3}}, \tag{A.41}$$

which we can recognise from comparison to Equation A.39 as

$$J_\mathrm{d} = \frac{1}{3}J_\mathrm{orb}. \tag{A.42}$$

After verifying that this is indeed a minimum, we can conclude that whatever changes happen to the system, a new stable solution can only be found for a state with a *higher* total angular momentum. Since no angular momentum can be imported, no stable solution is possible and the Darwin instability occurs.

B   References

Darwin, G. H. 1879, Proc. R. Soc., 29, 168 [LINK]

Dewi, J. D. M. & Tauris, T. M. 2000, A&A, 360, 1043 [ADS]

Eggleton, P. 2006, Evolutionary Processes in Binary and Multiple Stars

Eggleton, P. P. 1983, ApJ, 268, 368 [ADS]

Hjellming, M. S. & Webbink, R. F. 1987, ApJ, 318, 794 [ADS]

Loveridge, A. J., van der Sluys, M., & Kalogera, V. 2010, ArXiv e-prints [ADS]

Miller, J. M., Miller, M. C., & Reynolds, C. S. 2011, ApJL, 731, L5 [ADS]

Nauenberg, M. 1972, ApJ, 175, 417

Nelemans, G. & Tout, C. A. 2005, MNRAS, 356, 753 [ADS]

Nelemans, G., Verbunt, F., Yungelson, L. R., & Portegies Zwart, S. F. 2000, A&A, 360, 1011 [ADS]

Nelemans, G., Yungelson, L. R., Portegies Zwart, S. F., & Verbunt, F. 2001, A&A, 365, 491 [ADS]

Paczyński, B. 1967, Acta Astronomica, 17, 287 [ADS]

—. 1971, ARA&A, 9, 183 [ADS]

Paczynski, B. 1976, in IAU Symposium, Vol. 73, Structure and Evolution of Close Binary Systems, ed. P. Eggleton, S. Mitton, & J. Whelan, 75–+ [ADS]

Peters, P. C. 1964, Physical Review, 136, 1224 [ADS]

Sills, A., Pinsonneault, M. H., & Terndrup, D. M. 2000, ApJ, 534, 335 [ADS]

Soberman, G. E., Phinney, E. S., & van den Heuvel, E. P. J. 1997, A&A, 327, 620 [ADS]

Tauris, T. M. & Dewi, J. D. M. 2001, A&A, 369, 170 [ADS]

van der Sluys, M., Politano, M., & Taam, R. E. 2010, in American Institute of Physics Conference Series, Vol. 1314, American Institute of Physics Conference Series, ed. V. Kologera & M. van der Sluys, 13–18 [ADS]

van der Sluys, M. V. 2006, Formation and evolution of compact binaries (PhD thesis) [LINK]

van der Sluys, M. V., Verbunt, F., & Pols, O. R. 2005, A&A, 440, 973 [ADS]

—. 2006, A&A, 460, 209 [ADS]

Verbunt, F. & Zwaan, C. 1981, A&A, 100, L7 [ADS]

Webbink, R. F. 1984, ApJ, 277, 355 [ADS]

Wikipedia. 2021, Moment of inertia — Wikipedia, The Free Encyclopedia, accessed 2021-03-07 [LINK]

Woods, T. E., Ivanova, N., van der Sluys, M. V., & Chaichenets, S. 2012, ApJ, 744, 12 [ADS]